

# $\nu$ SpaceSim: A Comprehensive Simulation Package to Model the Optical and Radio Signals from Extensive Air Showers Induced by Cosmic Neutrinos and Measured by Space-based Experiments

John F. Krizmanic<sup>a,\*</sup> for the  $\nu$ SpaceSim Collaboration

<sup>a</sup>NASA/GSFC

Laboratory for Astroparticle Physics

8800 Greenbelt Rd, Greenbelt, Maryland 20771, USA

E-mail: [john.f.krizmanic@nasa.gov](mailto:john.f.krizmanic@nasa.gov)

*$\nu$ SpaceSim* is a comprehensive end-to-end simulation package created to facilitate the design of space-based and suborbital cosmic neutrino experiments that use the Earth as a neutrino converter as well as to understand the data obtained from current experiments.  *$\nu$ SpaceSim* models all aspects of the processes that lead to the neutrino-induced extensive air shower (EAS) signals: the modeling of neutrino interactions inside the Earth, propagating the leptons through the Earth into the atmosphere, modeling the tau-lepton decays, forming composite EAS, generating the air optical Cherenkov and radio signals, modeling their propagation and attenuation through the atmosphere. Finally, the response of optical and radio detectors is modeled.  *$\nu$ SpaceSim* uses a vectorized Python implementation to efficiently simulate neutrino-induced and background signals at a specific orbit or balloon altitude based on user xml input. The development has been focused on modeling the upward-moving EASs generated from Earth-emergent leptons sourced by neutrino interactions within the Earth, for both diffuse and transient sources accounting for the user-defined acceptance of an instrument. The tau-lepton channel is implemented using the modeling packages nuPyProp and nuLeptonSim. A MERRA-2 database driven application is used to generate cloud maps. Ionosphere dispersion of the radio signals is also modeled. In this paper, the  *$\nu$ SpaceSim* software, physics modeling, and the cosmic neutrino measurement capabilities of example experimental configurations will be presented.

38th International Cosmic Ray Conference (ICRC2023)  
26 July - 3 August, 2023  
Nagoya, Japan



---

\*Speaker

## 1. Overview

The measurement of the spectra and variability of the Very-High Energy (VHE:  $E_\nu \gtrsim 1$  PeV) cosmic neutrinos and their angular distribution on the sky provide a unique probe of high-energy astrophysical phenomena, especially in a multi-messenger astrophysics context. The importance of this has been explicitly stated in the Astro2020 Decadal Review [1], “*Astrophysical observations with non-EM messengers such as GWs[gravitational waves], neutrinos, and UHECRs[ultra-high energy cosmic rays] provide a new way to view the universe. Multimessenger astrophysics (MM), where these new observations are combined with more traditional data across the EM spectrum, opens enormous discovery space for understanding high-energy astrophysical sources, and provides new cosmological tools and tests of fundamental physics*” and in the 2022 Snowmass white paper on *High-Energy and Ultra-High-Energy Neutrinos* [2]. The results from IceCube [3, 4] demonstrate the existence of an extra-solar system astrophysical neutrino flux with neutrino energies from  $> 10$  TeV to potentially  $\sim 10$  PeV, including an event consistent with the Glashow resonance at 6.3 PeV [5]. Furthermore, recent results indicate a highly significant correlation with the Galactic plane and consistent with the distribution of gamma-ray sources [6]. The IceCube measurement of a significant excess of neutrinos at the location of the nearby active galaxy NGC 1068 provides evidence of an extra-galactic source [7]. The IceCube observation [8] of a neutrino coincident with gamma-rays from the blazar flare TXS 0506+056 and the hints of association with neutrino detections and Tidal Disruption Events [9, 10] demonstrate both the strength of MM astrophysics and the necessity to detect neutrino transient events. These results strengthen the case for development of sub-orbital Ultra-Long Duration Balloon (ULDB) experiments, such as EUSO-SPB2 [11] and the next generation of neutrino ULDB experiments, as well as space-based experiments, such as the Probe Of Extreme Multi-Messenger Astrophysics (POEMMA) mission [12] designed to measure the flux of cosmic neutrinos by using the Earth as an immense neutrino-converter and the atmosphere as the particle detector by measuring the optical and radio signals from extensive air showers (EAS). These scientific results provide the motivation for  *$\nu$ SpaceSim* which is to provide a comprehensive end-to-end simulation package to develop the next generation of EAS optical and radio sub-orbital and space-based cosmic neutrino instruments.

## 2. Current Simulation Version and Performance

The current version of  *$\nu$ SpaceSim* (v1.3.3) has been built upon the previous simulation work supporting ANITA [13, 14], SWORD [15], POEMMA [16–18], and EUSO-SPB2 [19, 20], to provide the first package that simultaneously simulates both the  $\nu$ -induced optical Cherenkov and radio EAS emission, atmospheric propagation, and instrument response based on well-defined user input parameters. Figs. 1 & 2 show the  *$\nu$ SpaceSim* HEASARC web portal, GitHub web portal, and a high-level flowchart detailing the  *$\nu$ SpaceSim* modeling structure. The current output provides data to calculate cosmic neutrino sensitivity of a defined instrument configuration while recording event-by-event analysis variables that can be displayed in histogram formats.

The  *$\nu$ SpaceSim* initial modeling effort has been focused on simulating the signals resulting from tau neutrino interactions in the Earth that lead to upward-moving EASs created by  $\tau$ -lepton decay. The  *$\nu$ SpaceSim* framework is shown functionally in Fig. 2. Originally, individual physics modules were written in high-level languages (Fortran, C, and C++) then wrapped in a vectorized Python scheduler, which retains high performance relative to the module languages. As the development has

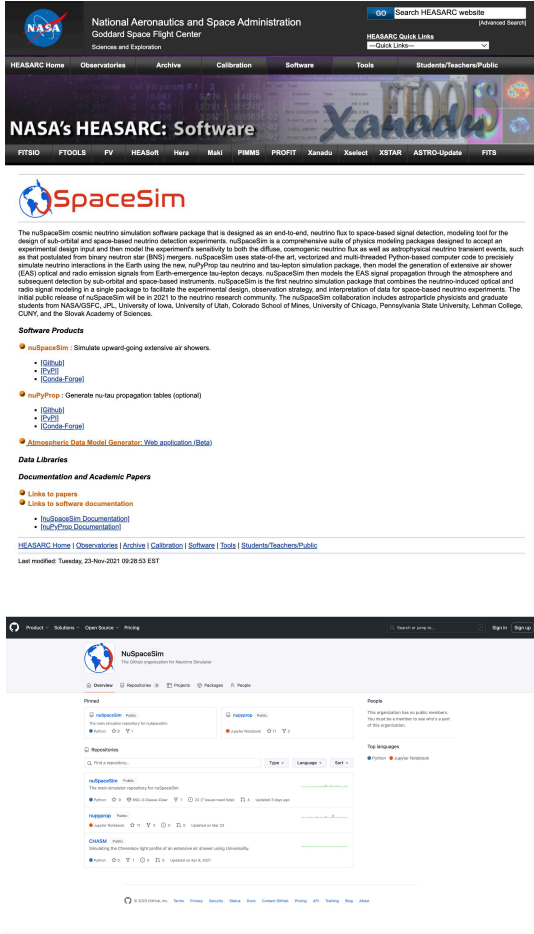


**Figure 1:** Top: Screenshot of the HEASARC vSpaceSim web portal detailing the links to vSpaceSim, nuPyProp, and the atmospheric data model generator based on the MERRA-2 database [21]. Bottom: The GitHub web page.

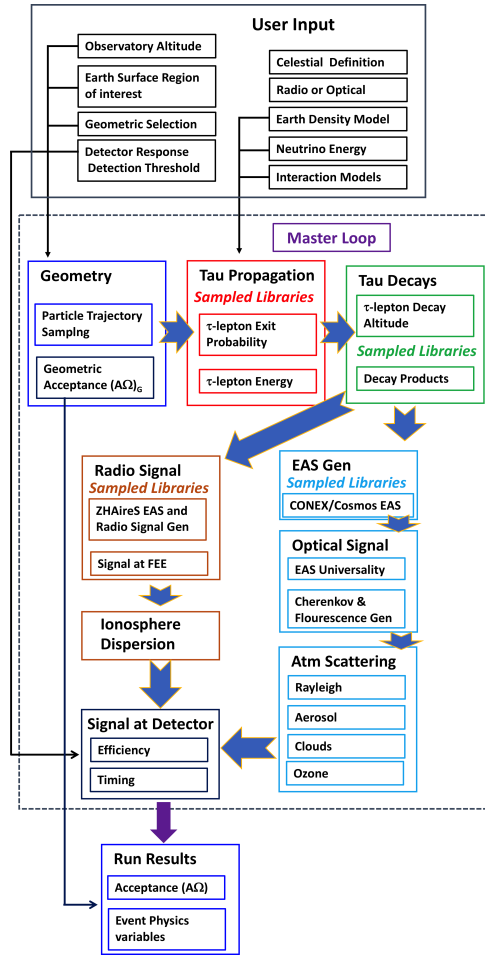


**Figure 2:** The vSpaceSim flowchart detailing the modular functionality of the simulation software package.

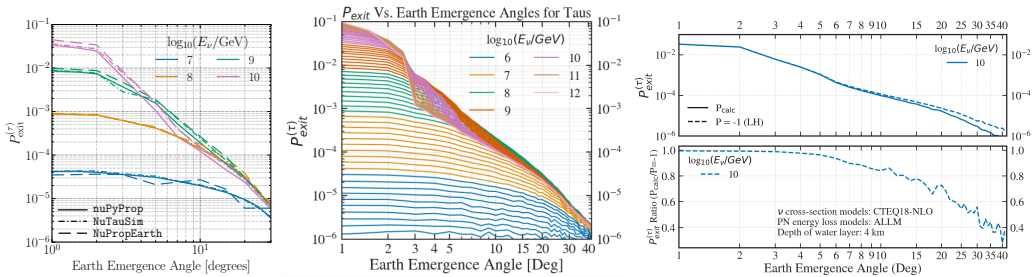


**Figure 3:** Left: A comparison of tau exit probabilities as a function of Earth emergence angle for nuPyProp, NuTauSim and NuPropEarth. Center: The  $\tau$ -lepton exit probabilities interpolated for a range of fixed incident neutrino energies between  $10^7 - 10^{12}$  GeV in tenth of decade cadence from nuPyProp, Right: Results for the tau exit probability for the impact of depolarization from electromagnetic scattering of  $\tau$ -leptons from from nuPyProp.

POS (ICRC2023) 1110

progressed, the modules in higher-level languages have been 'pythonized' to improved performance while retaining accuracy. Currently the performance on a MacBook Pro with a M2max processor is  $\sim 5$  minutes to generate  $10^6$  events with both optical and radio responses modeled. A sampled library approach is used to promptly generate simulated signals at a detector at a specific altitude whence a detector response module records the events. Pre-built libraries in the form of lookup tables are used for the more computationally intensive parts of the simulation (e.g., the  $\tau$ -lepton Earth-emergence probability distributions, the EAS longitudinal charge-particle profiles, the  $\tau$ -lepton decay channels, the EAS optical Cherenkov and radio signals, etc.). This allows the user to efficiently use the simulator to vary experimental parameters to optimize the design of a neutrino-detecting experiment.

The baseline physics modules include event and celestial geometry, sampling the  $\tau$ -lepton Earth-emergence probability distributions and energies, generation of the  $\tau$ -lepton decay location and products, sampling of EAS profile libraries, generation of the optical Cherenkov and radio EAS signals, propagation of the signals through the atmosphere (including attenuation of the Cherenkov light and ionosphere dispersion of the radio signals) and modeling the detector response. The pre-compiled package is available for public download via `pip` [22] and the open-source code is available via a public GitHub repository [23], which includes documentation and user issue reporting. Source-code tarballs of past releases are hosted by the HEASARC at GSFC.

For incident  $\nu_\tau$ , propagation through the Earth involves a series of neutrino interactions and  $\tau$ -lepton decays (regeneration), while for  $\nu_\mu$ , only a single  $\nu_\mu \rightarrow \mu$  interaction is required since muons lose so much energy in transit through the Earth. The default model to handle the propagation in  *$\nu$ SpaceSim* is `nuPyProp` [24]. However, the modular design allows to easily use other propagators with little effort, and a version of `nuSpaceSim` using `NuTauSim`/`NuLeptonSim` [25] is currently under development. Along with other publicly available neutrino propagation codes including including `TauRunner` [26, 27], and `nuPropEarth` [28]. Using different Earth-emergent lepton generators provides a quantification of the modeling systematic errors in this part of the simulation.

Here we provide the  *$\nu$ SpaceSim* input and simulation results of an example ULDB configuration that measures both the Optical Cherenkov and geomagnetic radio EAS signals from Earth-emergent  $\tau$ -leptons from tau neutrino interactions in the Earth. Fig. 4 presents the input xml input, in the left panel, for an experimental configuration at 33-km altitude with a  $1 \text{ m}^2$  optical collecting area and a 10-antennae radio configuration both viewing full azimuth and the Earth from the the limb to an angle  $6.4^\circ$  below the limb. The right panel of Fig. 4 shows the all-flavor diffuse neutrino sensitivity for Earth-emergent  $\tau$ -leptons assuming a 100-day observation, 20% optical duty cycle, and 100% radio duty cycle. No correlation between the measurements is assumed for these results.

### 3. Simulation Improvements under Development

To improve the fidelity of  *$\nu$ SpaceSim*, we are currently upgrading the modeling performance while keeping its highly efficient performance. These include modeling EAS development variability, updated Cherenkov light, radio, and timing calculations, the effects of clouds on optical signals, more versatile detector response models, and transient source (ToO) modeling. Future planned enhancements include optical and radio signals from muonic EAS, and UHECR backgrounds (including effects of atmospheric refraction), signals from EAS muon component from hadronic interactions forming the EAS, and support tool expansion, such as to aid in determining

```
<?xml version='1.0' encoding='UTF-8'?>
<NuSpaceSimParams>
  <DetectorCharacteristics Type="Satellite" Method="Both">
    <QuantumEfficiency>0.2</QuantumEfficiency>
    <TelescopeEffectiveArea Unit="Sq.Meters">1.0</TelescopeEffectiveArea>
    <PhotoElectronThreshold Preset="true">
      <NPE>40.0</NPE>
    </PhotoElectronThreshold>
    <DetectorAltitude Unit="km">33.0</DetectorAltitude>
    <InitialDetectorRightAscension Unit="Degrees">0.0</InitialDetectorRightAscension>
    <InitialDetectorDeclination Unit="Degrees">0.0</InitialDetectorDeclination>
    <LowFrequency Unit="MHz">30.0</LowFrequency>
    <HighFrequency Unit="MHz">300.0</HighFrequency>
    <SNRThreshold>5.0</SNRThreshold>
    <NAntennas>10</NAntennas>
    <AntennaGain>1.8</AntennaGain>
  </DetectorCharacteristics>
  <SimulationParameters DetectionMode="Diffuse">
    <MaximumCherenkovAngle Unit="Degrees">10.0</MaximumCherenkovAngle>
    <AngleFromLimb Unit="Degrees">6.4</AngleFromLimb>
    <TauShowerType Preset="true">
      <FracETauInShower>0.5</FracETauInShower>
    </TauShowerType>
    <NuTauEnergySpecType>
      <MonoSpectrum>
        <LogNuEnergy>7.0</LogNuEnergy>
      </MonoSpectrum>
    </NuTauEnergySpecType>
    <AzimuthalAngle Unit="Radians">6.283185307179586</AzimuthalAngle>
    <NumTrajs>1000000</NumTrajs>
    <ModelIonosphere>0</ModelIonosphere>
    <TEC>10.0</TEC>
    <TECerr>0.1</TECerr>
    <TauTableVer>3</TauTableVer>
  </SimulationParameters>
</NuSpaceSimParams>
```

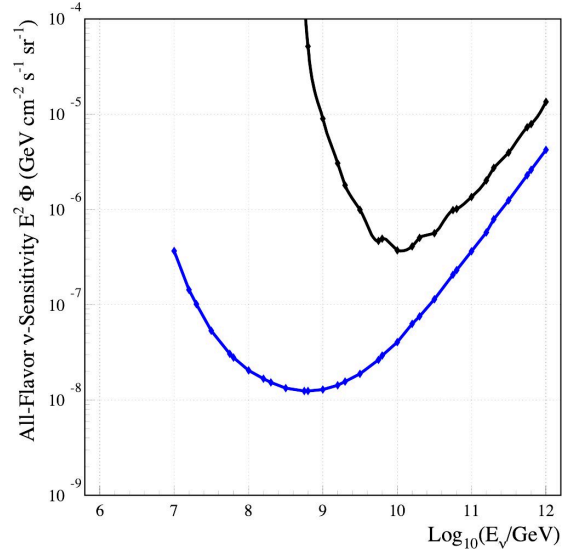


**Figure 4:** Left: Example xml input file for  $10^6$  events, 33 km altitude,  $\Delta_\alpha = 6.4^\circ$ ,  $\Delta_\phi = 360^\circ$ , detailing the optical and radio (with ionosphere dispersion turned off) simulation parameters. Right: All-flavor diffuse neutrino sensitivity results from *vSpaceSim* for the the detector configuration described in the xml example assuming a 100-day balloon flight at 33 km, with 20% duty cycle for the optical Cherenkov signal (blue curve) and 100% duty cycle for the geomagnetic radio measurements (black curve).

background effects on energy thresholds for the Cherenkov and radio configurations used in each simulation run. Here we detail some of these improvements.

**Improved Modeling of EAS Development from  $\tau$ -lepton Decay:** Results from CONEX [29] runs are shown in Fig. 5, with a comparison to the Greisen parameterization results, for upward-moving EASs from pions emitted at  $\beta_E = 5^\circ$  Earth-emergence angles. The results also show the EAS variability due to starting at various altitudes. These results demonstrate that EAS development can be highly suppressed at high altitudes due to the rarefied atmosphere. These effects necessitate the focus on high-altitude EAS modeling we have been performing in the

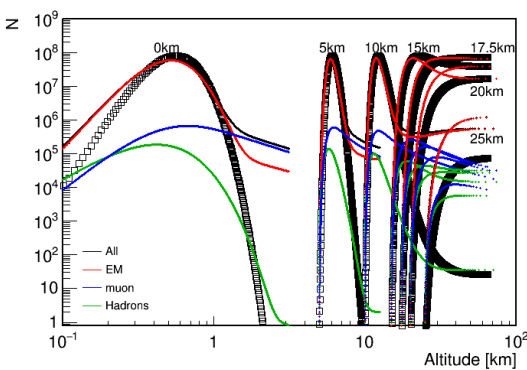


**Figure 5:** The average longitudinal EAS profiles from the CONEX simulation for 100 PeV pions (1000 events) for  $5^\circ$  Earth-emergence angle as a function of EAS starting altitudes. The various components are shown by the solid lines while the black boxes show the profile based from the Greisen parameterization for 100 PeV.

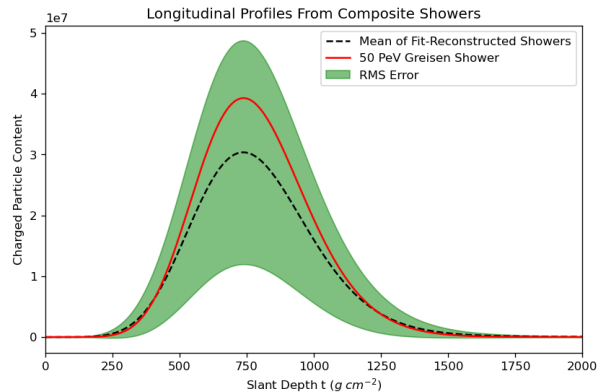


**Figure 6:** Comparison of the mean and variance of composite EAS formed from  $\tau$ -lepton decay products using PYTHIA 8 and CONEX parameterized component showers compared to the profile for a 100 PeV  $\tau$ -lepton decay currently in *vSpaceSim1.3.3*.

*vSpaceSim* development. Using the CONEX modeling of the evolution of the charged-particle content of EASs, composite EASs can be formed using the specific decay products provided in the PYTHIA [30]  $\tau$ -lepton decay libraries. Fig. 6 shows the results of forming composite EAS (starting at sea level and at  $\beta_E = 5^\circ$ ) showing the mean, RMS variation, and comparison to a Greisen EAS at the appropriate energy. This modeling is currently being implemented in *vSpaceSim*.

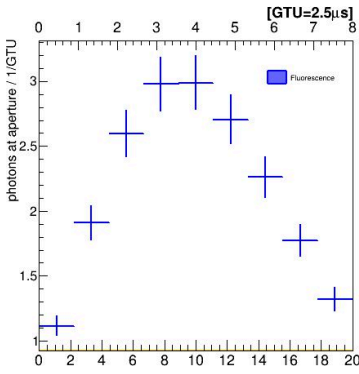
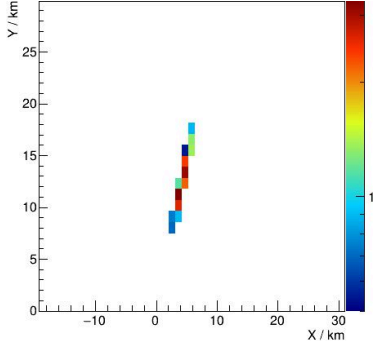


**Figure 7:** The EUSO-Offline results for a 1 EeV  $\nu_\tau$  that led to a 0.7 EeV upward-moving EAS with a  $17^\circ$  Earth-emergence angle as recorded by a POEMMA instrument model ( $\sim 6\text{-m}^2$  optical aperture, nadir pointing at 525 km altitude, and  $2.5\ \mu\text{s}$  GTU time). The integrated fluorescence signal on the optical aperture is  $\sim 20,000$  photons.

Along these lines, the EAS longitudinal profiles for the upward-moving EAS developed in *vSpaceSim* can be generated in a CONEX output format to be used as input to other experiments, thus providing simulation results for upward-moving EAS generated at arbitrary starting altitude. As an example, Fig. 7 shows the results of the EUSO-Offline simulation [31] assuming a single, nadir-pointed POEMMA instrument, using the profile of a *vSpaceSim* generated 0.7 EeV upward-moving EAS that was created by a 1 EeV neutrino interacting in the Earth. The results show a detection on POEMMA’s fluorescence camera.

**Effects of Clouds on the EAS Optical Cherenkov:** We are currently extending the atmospheric modeling of *vSpaceSim* by including the effects of clouds on the propagation of the EAS optical signals. This new feature is currently being validated and should be available in the near term and assumes clouds are optically thick and only the portion of the EAS above a cloud can contribute Cherenkov light. Currently, three cloud options are available: a no-cloud option, a constant cloud layer at a specific altitude, and cloud layer distributions obtained using the data products available in the MERRA-2 database [21]. Fig. 8 presents the impact of clouds on the instantaneous  $\nu_\tau$  aperture for the balloon-borne instrument with the parameters in Fig. 4. The results show that while clouds do modify the acceptance of optical Cherenkov events, the MERRA-2 case has much smaller reduction than a constant cloud layer with a 5 km height.

**Higher Fidelity Modeling of the Optical Cherenkov Light Generation using CHASM:** CHASM [32] is a python package which leverages the universality of charged particles in an extensive air shower to produce a deterministic prediction of the Cherenkov light for a given shower profile and geometry. CHASM accesses pre-compiled tables of Cherenkov angular and yield distributions for each stage of shower development with the flexibility to model both downward- and upward-moving EAS. CHASM uses CORSIKA’s atmospheric extinction tables to calculate extinction along Cherenkov photon travel paths. Fig. 9 shows the signal of ANEAS at an array of counters in orbit facing normal to the shower axis. Since these types EAS will be highly inclined, the curvature of the atmosphere has a significant effect. Fig. 10 shows the arrival time distribution at just one counter for the same EAS both with and without the CHASM curved atmosphere treatment.

POS (ICRC2023) 1110

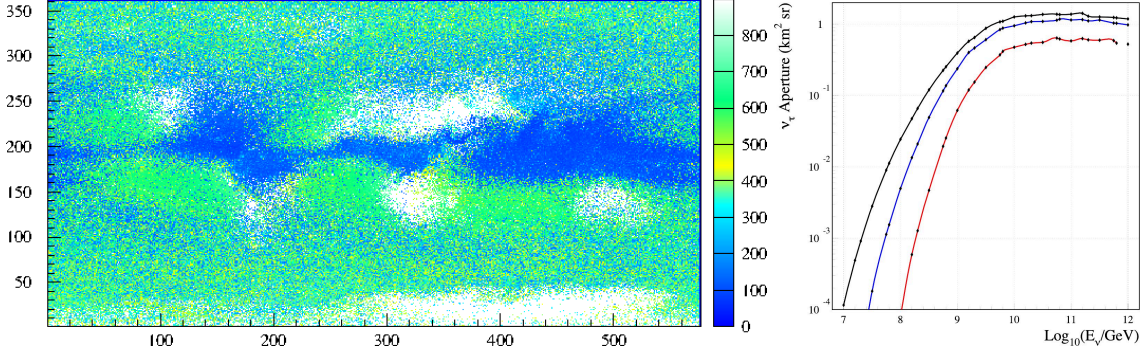


**Figure 8:** Left: The 10-year-averaged cloud distribution for June obtained from the MERRA-2 database. The axes show the bin number while the color code is cloud-top pressure in torr. Right: The instantaneous  $\nu_\tau$ -aperture for a EUSO-SPB2-like instrument defined by the parameters presented in Fig. 4. The black line shows the  $\nu_\tau$ -aperture for the no-cloud condition, blue line shows that for the MERRA-2 cloud distribution in the left panel positioned at (Lat= 0°, Long= 0°), and the red line is the  $\nu_\tau$ -aperture assuming a continuous layer of clouds at an altitude of 5 km. The results of the constant altitude cloud case are consistent with that from a previous study [17].

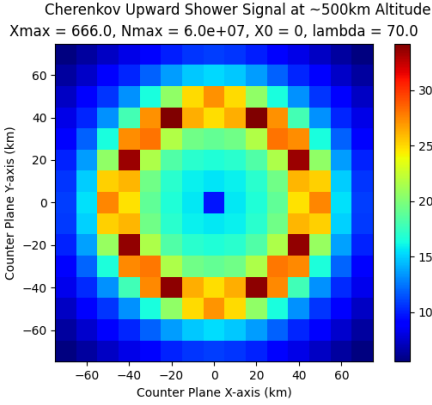


**Figure 9:** Upward going shower signal from CHASM with 85 degree zenith angle.

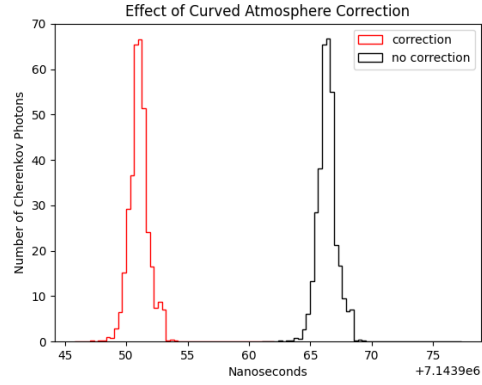


**Figure 10:** Arrival time distribution predicted by CHASM.

#### 4. Summary and Acknowledgements

*$\nu$ SpaceSim* has provided an end-to-end cosmic neutrino simulation model that successfully models both the optical Cherenkov and geomagnetic radio signals generated from  $\tau$ -lepton decays induced from tau neutrino interactions within the Earth. In this paper, some of the continuing development we are enacting to provide the community with the improvements in both modeling fidelity and functionality are presented. This work is supported by NASA RTOP 21-APRA21-0071 at NASA/GSFC and NASA grants 80NSSC22K1520 at the University of Chicago, 80NSSC22K1517 at the Colorado School of Mines, 80NSSC22K1523 at the University of Iowa, 80NSSC22K1519 at Pennsylvania State University, and 80NSSC22K1522 at the University of Utah.

#### References

- [1] *Pathways to Discovery in Astronomy and Astrophysics for the 2020s* (National Academies of Sciences · Engineering · Medicine, 2021).
- [2] M. Ackermann, M. Bustamante, L. Lu, N. Otte, M. H. Reno, S. Wissel, M. Ackermann, S. K. Agarwalla, J. Alvarez-Muñiz, R. Alves Batista, et al., *Journal of High Energy Astrophysics* **36**, 55 (2022), 2203.08096.

- [3] M. G. Aartsen et al., *Advances in Space Research* **62**, 2902 (2018), [1701.03731](#).
- [4] M. G. Aartsen et al., *Phys. Rev. D* **98**, 062003 (2018).
- [5] M. G. Aartsen et al., *Nature* **591**, 220 (2021).
- [6] Icecube Collaboration, R. Abbasi, M. Ackermann, J. Adams, J. A. Aguilar, M. Ahlers, M. Ahrens, J. M. Alameddine, A. A. Alves, N. M. Amin, et al., *Science* **380**, 1338 (2023), [2307.04427](#).
- [7] IceCube Collaboration, R. Abbasi, M. Ackermann, J. Adams, J. A. Aguilar, M. Ahlers, M. Ahrens, J. M. Alameddine, C. Alispach, J. Alves, A. A., et al., *Science* **378**, 538 (2022), [2211.09972](#).
- [8] M. G. Aartsen et al., *Science* **361**, eaat1378 (2018), [1807.08816](#).
- [9] R. Stein and other, *Nature Astronomy* **5**, 510 (2021), [2005.05340](#).
- [10] S. Reusch, R. Stein, M. Kowalski, S. van Velzen, A. Franckowiak, C. Lunardini, K. Murase, W. Winter, J. C. A. Miller-Jones, M. M. Kasliwal, et al., *Phys. Rev. Lett.* **128**, 221101 (2022).
- [11] J. Eser, L. Olinto, Angela V. Wiencke, et al., *Overview and First Results of EUSO-SPB2* (2023).
- [12] A. V. Olinto, J. F. Krizmanic, et al., *Journal of Cosmology and Astroparticle Physics* **2021**, 007 (2021).
- [13] A. Romero-Wolf et al., *Phys. Rev. D* **99**, 063011 (2019), [1811.07261](#).
- [14] R. Prechelt, S. A. Wissel, A. Romero-Wolf, C. Burch, P. W. Gorham, P. Allison, J. Alvarez-Muñiz, O. Banerjee, L. Batten, J. J. Beatty, et al., "Phys. Rev. D", **105**, 042001 (2022), [2112.07069](#).
- [15] A. Romero-Wolf, P. Gorham, K. Liewer, J. Booth, and R. Duren, *ArXiv e-prints* (2013), [1302.1263](#).
- [16] L. A. Anchordoqui et al., *Phys. Rev. D* **101**, 023012 (2020).
- [17] M. H. Reno, J. F. Krizmanic, and T. M. Venters, *Phys. Rev. D* **100**, 063010 (2019).
- [18] T. M. Venters, M. H. Reno, J. F. Krizmanic, L. A. Anchordoqui, C. Guépin, and A. V. Olinto, *Phys. Rev. D* **102**, 123013 (2020).
- [19] A. L. Cummings, R. Aloisio, and J. F. Krizmanic, *Phys. Rev. D* **103**, 043017 (2021), [2011.09869](#).
- [20] A. L. Cummings, R. Aloisio, J. Eser, and J. F. Krizmanic, "Phys. Rev. D", **104**, 063029 (2021), [2105.03255](#).
- [21] R. Gelaro, W. McCarty, M. J. Suarez, R. Todling, A. Molod, L. Takacs, C. A. Randles, A. Darnenov, M. G. Bosilovich, R. Reichle, et al., *Journal of Climate* **30**, 5419 (2017).
- [22] A. Reustle et al. (NuSpaceSim), *nuSpaceSim pypi (pip) webpage*, <https://pypi.org/project/nuspacesim/> (2021).
- [23] A. Reustle et al. (NuSpaceSim), *nuSpaceSim github repository*, <https://github.com/NuSpaceSim/nuSpaceSim> (2021).
- [24] D. Garg, S. Patel, M. H. Reno, A. Reustle, Y. Akaike, L. A. Anchordoqui, D. R. Bergman, I. Buckland, A. L. Cummings, J. Eser, et al., *JCAP* **2023**, 041 (2023), [2209.15581](#).
- [25] J. Alvarez-Muñiz, W. R. Carvalho, A. L. Cummings, K. Payet, A. Romero-Wolf, H. Schoorlemmer, and E. Zas, *Phys. Rev. D* **97**, 023021 (2018), [Erratum: *Phys.Rev.D* 99, 069902 (2019)], [1707.00334](#).
- [26] I. Safa, A. Pizzuto, C. A. Argüelles, F. Halzen, R. Hussain, A. Kheirandish, and J. Vandenbroucke, *JCAP* **01**, 012 (2020), [1909.10487](#).
- [27] I. Safa, J. Lazar, A. Pizzuto, O. Vasquez, C. A. Argüelles, and J. Vandenbroucke (2021), [2110.14662](#).
- [28] A. Garcia, R. Gauld, A. Heijboer, and J. Rojo, *JCAP* **09**, 025 (2020), [2004.04756](#).
- [29] T. Pierog, M. K. Alekseeva, T. Bergmann, V. Chernatkin, R. Engel, D. Heck, N. N. Kalmykov, J. Moyon, S. Ostapchenko, T. Thouw, et al., *Nuclear Physics B Proceedings Supplements* **151**, 159 (2006), [astro-ph/0411260](#).
- [30] T. Sjöstrand, S. Ask, J. R. Christiansen, R. Corke, N. Desai, P. Ilten, S. Mrenna, S. Prestel, C. O. Rasmussen, and P. Z. Skands, *Computer Physics Communications* **191**, 159 (2015), [1410.3012](#).
- [31] T. C. Paul (JEM-EUSO), *PoS ICRC2023*, 220 (2023).
- [32] I. J. Buckland and D. R. Bergman, *Astroparticle Physics* **150**, 102832 (2023).



**vSpaceSim Collaboration**

John Krizmanic<sup>1</sup>, Yosui Akaike<sup>2</sup>, Luis Anchordoqui<sup>3</sup>, Douglas Bergman<sup>4</sup>, Isaac Buckland<sup>4</sup>, Jorge Caraca-Valente<sup>5</sup>, Austin Cummings<sup>6</sup>, Johannes Eser<sup>7</sup>, Fred Angelo Batan Garcia<sup>1,9</sup>, Diksha Garg<sup>9</sup>, Claire Guépin<sup>10</sup>, Tobias Heibges<sup>5</sup>, Andrew Ludwig<sup>11</sup>, Simon Mackovjak<sup>12</sup>, Eric Mayotte<sup>5</sup>, Sonja Mayotte<sup>5</sup>, Angela Olinto<sup>7</sup>, Thomas Paul<sup>3</sup>, Alex Reustle<sup>1,13</sup>, Andrew Romero-Wolf<sup>11</sup>, Mary Hall Reno<sup>9</sup>, Fred Sarazin<sup>5</sup>, Tonia Venters<sup>1</sup>, Lawrence Wiencke<sup>5</sup>, Stephanie Wissel<sup>6</sup>

<sup>1</sup>NASA/Goddard Space Flight Center, Greenbelt, Maryland 20771 USA, <sup>2</sup>Waseda Institute for Science and Engineering, Waseda University, Shinjuku, Tokyo, Japan, <sup>3</sup>Department of Physics and Astronomy, Lehman College, City University of New York, New York, New York, 10468 USA, <sup>4</sup>Department of Physics and Astronomy, University of Utah, Salt Lake City, Utah 84112 USA, <sup>5</sup>Department of Physics, Colorado School of Mines, Golden, Colorado 80401 USA <sup>6</sup>Department of Physics, Pennsylvania State University, State College, Pennsylvania 16801 USA, <sup>7</sup>Department of Astronomy and Astrophysics University of Chicago, Chicago, Illinois 60637 USA, <sup>8</sup>Department of Physics and Astronomy, University of Iowa, Iowa City, Iowa 52242 USA, <sup>9</sup>Department of Astronomy, University of Maryland, College Park, College Park, Maryland 20742 USA, <sup>10</sup>Laboratoire Univers et Particules de Montpellier (LUPM), Université Montpellier, Montpellier Cedex 5, France, <sup>11</sup>Jet Propulsion Laboratory, California Institute of Technology, Pasadena, California 91109, USA, <sup>12</sup>Institute of Experimental Physics, Slovak Academy of Sciences, Kosice, Slovakia, <sup>13</sup>ADNET Systems.